Progress In Electromagnetics Research, PIER 79, 47–58, 2008

SCATTERING FROM SEMI-ELLIPTIC CHANNEL LOADED WITH IMPEDANCE ELLIPTICAL CYLINDER

M. M. Zahedi and M. S. Abrishamian

K. N. Toosi University of Technology
Electrical Engineering Department
P.O. Box 16315-1355, Tehran 16314, Iran

Abstract—Analytical TM scattering from semi-elliptic channel loaded with confocal elliptic cylindrical impedance core is investigated. Fields in every regions are expressed appropriately in terms of Mathieu functions. Applying boundary conditions at the impedance core and across different regions of channels and using orthogonality of angular Mathieu functions result in two simultaneous set of equations which would be solved numerically.

1. INTRODUCTION

Scattering from geometries with channels, grooves and cracks have received considerable attention due to fact that these local guiding structures may excite internal resonances which may have dramatic effects on the nearby electromagnetic structures. The electromagnetic scattering from semi-circular channel has been investigated in [1, 2] based on dual series eigenfunction solution. Later, this method has been applied to semi-elliptical channel in perfect conducting ground plane [3]. Others have used this method to investigate scattering of - Gaussian beam from semi-circular channel [4], semi-circular channel loaded with conducting and dielectric cylindrical core [5] and lately conducting elliptical core loading semi-elliptic cannel [6]. Also there have been other reports based on numerical solution [7, 8]. This paper presents analytical solution of scattering from impedance elliptical core loading confocally semi-elliptic channel. Effects of geometrical properties and reactance variation would be investigated.

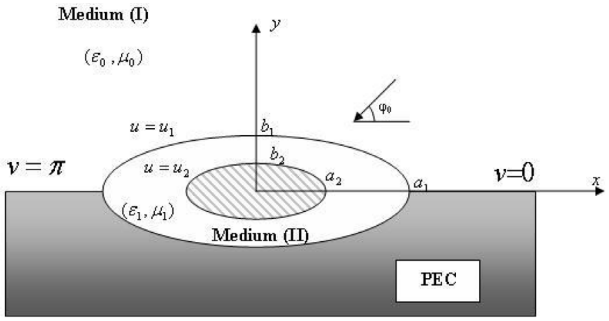

Figure 1. Geometry of the scattering problem.

2. FORMULATION

A linearly polarized electromagnetic plane wave is incident at an angle ϕ_0 with respect to $x-$axis, on the structure shown in Fig. 1, in which free space region is labeled medium I and dielectric region is labeled medium II. For the TM case, the electric field, in each region, has only axial component E_z which may be written as[†]

$$E_z^{inc} = e^{ik_0(x\cos\phi_0 + y\sin\phi_0)} \tag{1}$$

For structures involving elliptical shaped objects, it is customary to express field quantities in elliptic cylindrical coordinates (u, v, z), where $x = F\cosh u\cos v$, $y = F\sinh u\sin v$. The incident electric field, in terms of angular and radial Mathieu functions may be written in the form [9]

$$\begin{aligned} e^{ik_0(x\cos\phi_0 + y\sin\phi_0)} &= \sum_{n=0}^{\infty} 2\, i^n\, Mc_n^{(1)}(u, q_0)\, ce_n(\phi_0, q_0)\, ce_n(v, q_0) \\ &\quad + \sum_{n=1}^{\infty} 2\, i^n\, Ms_n^{(1)}(u, q_0)\, se_n(\phi_0, q_0)\, se_n(v, q_0) \end{aligned} \tag{2}$$

where $q_0 = (k_0F/2)^2$, $k_0 = \omega\sqrt{\epsilon_0\mu_0}$, ce_n and se_n are, respectively, the even and odd angular Mathieu functions of order n, $Mc_n^{(1)}$ and $Ms_n^{(1)}$ are even and odd radial Mathieu functions of first kind [10]. Scattered field in the region outside semi-elliptic channel $(u > u_1)$ is decomposed into specularly reflected and diffracted field [3, 6]. By taking into account that sum of the incident and scattered electric field

[†] $e^{i\omega t}$ time convention is assumed and suppressed.

must vanish at $v = 0$ and $v = \pi$ the total electric field in free space region (medium I), may be written as

$$\begin{aligned} E_z^{(I)}(u,v) &= E_z^{inc} + E_z^{diff} + E_z^{ref} \\ &= \sum_{n=1}^{\infty} B_n^{(s)}\, Ms_n^{(4)}(u,q_0)\, se_n(v,q_0) \\ &+ \sum_{n=1}^{\infty} 4\, i^n\, Ms_n^{(1)}(u,q_0)\, se_n(\phi_0,q_0)\, se_n(v,q_0) \end{aligned} \tag{3}$$

where $B_n^{(s)}$ is unknown scattered field coefficient and $Ms_n^{(4)}$ is the Mathieu function which corresponds to Hankel function of the second kind in circular coordinates and has the relationship of $Ms_n^{(4)} = Ms_n^{(1)} - i\, Ms_n^{(2)}$. In (3), E_z^{diff} and E_z^{ref} have been taken as

$$E_z^{diff}(u,v) = \sum_{n=1}^{\infty} B_n^{(s)}\, Ms_n^{(4)}(u,q_0)\, se_n(v,q_0) \tag{4}$$

$$E_z^{ref}(u,v) = -E_z^{inc}(u,v) \text{ with } \phi_0 \to 2\,\pi - \phi_0 \tag{5}$$

The electric filed inside the elliptical channel is expanded in terms of Mathieu functions as

$$\begin{aligned} E_z^{(II)} &= \sum_{n=0}^{\infty} \left[Ae_n^{(II)} Mc_n^{(1)}(u,q_1) + Be_n^{(II)} Mc_n^{(2)}(u,q_1) \right] ce_n(v,q_1) \\ &+ \sum_{n=1}^{\infty} \left[Ao_n^{(II)} Ms_n^{(1)}(u,q_1) + Bo_n^{(II)} Ms_n^{(2)}(u,q_1) \right] se_n(v,q_1) \end{aligned} \tag{6}$$

where $q_1 = (k_1 F/2)^2$, $k_1 = \omega\sqrt{\epsilon_1 \mu_1}$ and $Mc_n^{(2)}$, $Ms_n^{(2)}$ are radial Mathieu functions of second kind. From Maxwell postulates, the $v-$components of magnetic field may be represented as

$$H_v^{(I),(II)}(u,v) = \frac{-i}{\omega \mu_0 h_v} \frac{\partial E_z^{(I),(II)}}{\partial u} \tag{7}$$

where $h_v = F\sqrt{\cosh^2 u - \cos^2 v}$. Unknown coefficients $Be_n^{(I)}$ and $Bo_n^{(I)}$ in (6) may be eliminated by applying boundary condition on the surface of impedance elliptic cylinder ($u = u_2$) which can be written

$$E_z^{(II)}(u_2,q_1) = Z_s(v)\, H_v^{(II)}(u_2,q_1) \tag{8}$$

In (8) the surface impedance Z_s is assumed to be independent of axial direction z.

For a perfectly conducting cylinder coated with an imperfectly conducting or absorbing layer of thickness Δ and relative permittivity and permeability ϵ_c and μ_c, the surface impedance on the outer surface of a thin coating is given by [11]

$$Z_s(v) = ik_1\Delta(v)\mu_c Z_1 \tag{9}$$

where Z_1 is the characteristic impedance of the dielectric region wherein impedance surface is located. For a thin coating, $\Delta(v)$ can be expanded in terms of metric coefficient h_v and δu, a small variation of u about u_2 [12]. Thus surface impedance can be written as

$$Z_s(v) = \eta_s(\cosh^2 u_2 - \cos^2 v)^{1/2} Z_1 \tag{10}$$

where $\eta_s = 2\,i\sqrt{q_1}\,\mu_c\,\delta u_2\,\sinh u_2/(\cosh^2 u_2 - 1)$ is a complex quantity. Substituting $E_z^{(II)}$ and $H_v^{(II)}$ into (8) and using orthogonality of angular Mathieu functions over $[0, 2\pi]$ interval, the electric field in region (II) may be expressed as

$$E_z^{(II)} = \sum_{n=0}^{\infty} Me_n(u,q_1)ce_n(v,q_1) + \sum_{n=1}^{\infty} Mo_n(u,q_1)se_n(v,q_1) \tag{11}$$

where

$$Me_n(u,q_1) = Mc_n^{(1)}(u,q_1) - Pe_n\,Mc_n^{(2)}(u,q_1) \tag{12}$$

$$Mo_n(u,q_1) = Ms_n^{(1)}(u,q_1) - Po_n\,Ms_n^{(2)}(u,q_1) \tag{13}$$

and

$$Pe_n = \frac{Mc_n^{(1)}(u_2,q_1) + \dfrac{i\eta_s}{2\sqrt{q_1}} Mc_n^{(1)'}(u_2,q_1)}{Mc_n^{(2)}(u_2,q_1) + \dfrac{i\eta_s}{2\sqrt{q_1}} Mc_n^{(2)'}(u_2,q_1)} \tag{14}$$

$$Po_n = \frac{Ms_n^{(1)}(u_2,q_1) + \dfrac{i\eta_s}{2\sqrt{q_1}} Ms_n^{(1)'}(u_2,q_1)}{Ms_n^{(2)}(u_2,q_1) + \dfrac{i\eta_s}{2\sqrt{q_1}} Ms_n^{(2)'}(u_2,q_1)} \tag{15}$$

In (12) and (13) when $\eta_s = 0$, the expressions for $Me_n(u,q_1)$ and $Mo_n(u,q_1)$ become

$$Me_n(u,q_1)\Big|_{\eta_s=0} = Mc_n^{(1)}(u,q_1) - \frac{Mc_n^{(1)}(u_2,q_1)}{Mc_n^{(2)}(u_2,q_1)}\,Mc_n^{(2)}(u,q_1) \tag{16}$$

$$Mo_n(u,q_1)\Big|_{\eta_s=0} = Ms_n^{(1)}(u,q_1) - \frac{Ms_n^{(1)}(u_2,q_1)}{Ms_n^{(2)}(u_2,q_1)}\,Ms_n^{(2)}(u,q_1) \tag{17}$$

Thus the z-component of electric field expression in the case of $\eta_s = 0$ is the same as reported in [6].

Other unknown coefficients $Ae_n^{(II)}$, $Ao_n^{(II)}$ and $B_n^{(s)}$ can be determined with boundary conditions at $u = u_1$ of zero tangential electric field on the channel ($\pi < v < 2\pi$) and tangential fields continuity across the aperture ($0 < v < \pi$). Applying orthogonality condition of angular Mathieu functions and eliminating $Ao_n^{(II)}$, simultaneous equations may be obtained which in block matrix form can be written as

$$\begin{pmatrix} \mathbf{A}_{mn} & \mathbf{B}_{mn} \\ \mathbf{C}_{mn} & \mathbf{D}_{mn} \end{pmatrix} \begin{pmatrix} \mathbf{Ao}_m^{(II)} \\ \mathbf{B}_m^{(s)} \end{pmatrix} = \begin{pmatrix} \mathbf{G}_m \\ \mathbf{H}_m \end{pmatrix} \tag{18}$$

where

$$\mathbf{A}_{mn} = 2\, Me_n(u_1, q_1)\, I_{mn}^{sc}(q_1, q_1) \tag{19}$$

$$\mathbf{B}_{mn} = -Ms_n^{(4)}(u_1, q_0)\, I_{mn}^{ss}(q_1, q_0) \tag{20}$$

$$\mathbf{C}_{mn} = \left[Me_n^{'}(u_1, q_1) + \Delta_{om}\, Me_n(u_1, q_1)\right]\, I_{mn}^{sc}(q_1, q_1) \tag{21}$$

$$\mathbf{D}_{mn} = -\frac{\mu_1}{\mu_0} Ms_n^{(4)^{'}}(u_1, q_0)\, I_{mn}^{ss}(q_1, q_0) \tag{22}$$

$$\mathbf{G}_m = \sum_{n=1}^{\infty} 4\, i^n\, Ms_n^{(1)}(u_1, q_0)\, se_n(\phi_0, q_0)\, I_{mn}^{ss}(q_1, q_0) \tag{23}$$

$$\mathbf{H}_m = \frac{\mu_1}{\mu_0} \sum_{n=1}^{\infty} 4\, i^n\, Ms_n^{(1)^{'}}(u_1, q_0)\, se_n(\phi_0, q_1)\, I_{mn}^{ss}(q_1, q_0) \tag{24}$$

$$\Delta_{om} = \frac{Mo_m^{'}(u_1, q_1)}{Mo_m(u_1, q_1)} \tag{25}$$

and

$$I_{mn}^{sc}(q_1, q_2) = \int_0^{\pi} se_m(v, q_1)\, ce_n(v, q_2)\, dv \tag{26}$$

$$I_{mn}^{ss}(q_1, q_2) = \int_0^{\pi} se_m(v, q_1)\, se_n(v, q_2)\, dv \tag{27}$$

Normalization integrals (26) and (27) can be expressed in terms of Mathieu expansion coefficients and is given in appendix A.

3. NUMERICAL RESULTS

Once unknown coefficients are known all near and far field quantities can be calculated. The scattered far field at very large distances from

semi-elliptical structure may be deduced by noting that at far zone, the following limits can be made

$$\lim_{u\to\infty} 2\sqrt{q}\cosh u = k_0\rho, \quad \text{and} \quad v \to \phi \tag{28}$$

where ρ is cylindrical radial distance. Using the above limiting values, the expression for E_z^{diff} at large distances is given by

$$E_z^{diff} = \sqrt{\frac{2\,i}{\pi k_0 \rho}}\, e^{-ik_0\rho} F(v, q_0) \tag{29}$$

where the far field pattern is

$$F(v, q_0) = \sum_{n=1}^{\infty} i^n\, B_n^{(s)} se_n(\phi, q_0) \tag{30}$$

To check the validity and accuracy of the propose method and computation, far field pattern of present geometry with small eccentricities ($e = 0.01$) with $\eta_s = 0$ was computed versus channel electrical size variation and is shown in Fig. 2. Excellent agreement between all results is apparent except for one point which may be attributed to approximating a large circle ($a_1 = 2\,\lambda_0$) by an ellipse of small eccentricity.

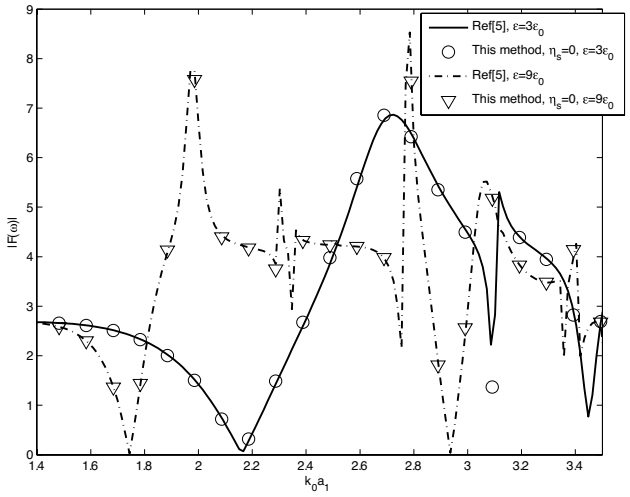

Figure 2. Far field pattern for core loaded semi-elliptic channel with $a_2 = 0.2\,\lambda_0$, $e = 0.01$ and $\eta_s = 0$ versus channel electrical size.

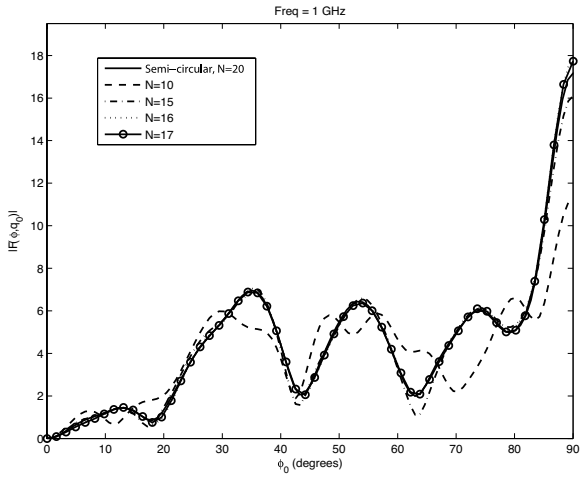

Figure 3. Far field pattern for loaded semi-elliptic channel with $\epsilon = 3\epsilon_0$, $a_2 = \lambda_0$, $a_1 = 2\,\lambda_0$, $e = 0.01$ and $\eta_s = 0$ versus incident angle.

In order to solve for the unknown field coefficients, the infinite block matrix system of equations (18) must be truncated appropriately for convergence. In order to study convergence of infinite system of equations, two problems are considered. First the convergence for the case of small eccentricity. Fig. 3 demonstrates the dependance of angular distribution of far field pattern of a loaded semi-elliptic channel with small eccentricity and $a_1 = 2\lambda_0$, $a_2 = \lambda_0$ for different number of truncation terms N. For $N = 16$ and $N = 17$ semi-elliptic curves converge to semi-circular one except for some critical points which is the result of small eccentricity approximation for such a fairly large structure. Any further increase in N results in singularity of block matrix (18) due to rapidly vanishing property of Mathieu functions. Fig. 4 is the dependance of angular distribution of far field pattern of a loaded semi-elliptic channel with $e = 0.5$ and $\epsilon = 4\epsilon_0$ for different number of truncation terms. It is apparent that the curves for $N = 24$ and $N = 25$ are completely overlapped, which means the matrix equation (18) is convergent for $N = 25$ which corresponds to $2k_0a_1$. Fig. 5 is as same as Fig. 4 except for $\eta_s = 0.5 - 0.5i$ and demonstrates the independency of number of truncation terms on surface impedance value. It has been found through lots of simulations that $N = 2k_0a_1$ is sufficient for most problems excluding extreme cases such as small eccentricity or very high permittivity and is independent of surface impedance.

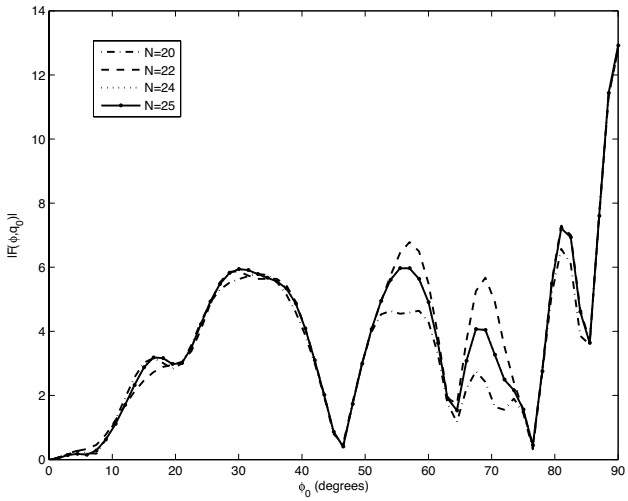

Figure 4. Far field pattern for loaded semi-elliptic channel with $\epsilon = 4\epsilon_0$, $a_2 = \lambda_0$, $a_1 = 2\,\lambda_0$, $e = 0.5$ and $\eta_s = 0$ versus incident angle for different truncation terms.

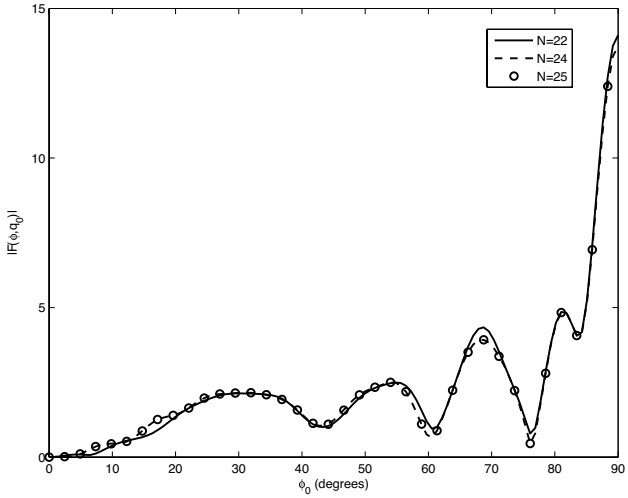

Figure 5. Far field pattern for loaded semi-elliptic channel with $\epsilon = 4\epsilon_0$, $a_2 = \lambda_0$, $a_1 = 2\,\lambda_0$, $e = 0.5$ and $\eta_s = 0.5 - 0.5i$ versus incident angle.

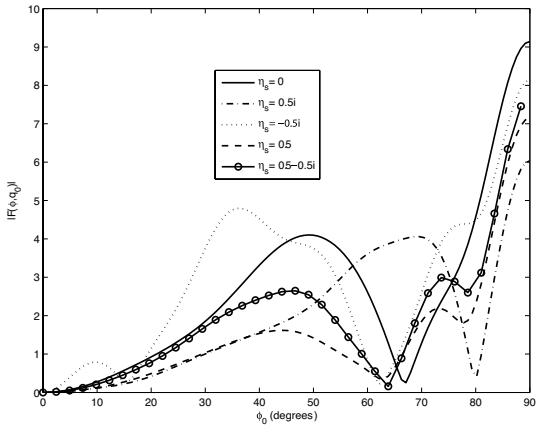

Figure 6. Far field pattern for loaded semi-elliptic channel with $\epsilon = 4\epsilon_0$, $a_2 = 0.7\lambda_0$, $a_1 = \lambda_0$, $e = 0.5$ versus incident angle.

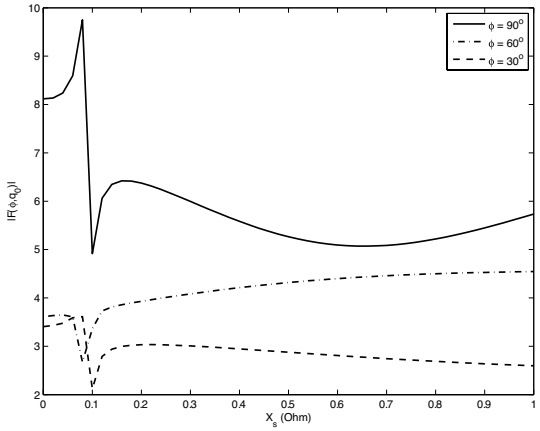

Figure 7. Far field pattern for loaded semi-elliptic channel with $\epsilon = 3\epsilon_0$, $a_2 = 0.7\lambda_0$, $a_1 = \lambda_0$, $e = 0.5$ versus surface reactance.

Fig. 6 shows the dependence of the backscattered field on the angle of incidence for different surface impedances. For all direction of incidence, it is apparent that both conducting ($\eta_s = 0.5 - 0.5i$) and resistive ($\eta_s = 0.5$) coatings tend to decrease the backscattering compared with the perfectly conducting case with no coating. However, an inductive coating ($\eta_s = 0.5i$) tends, for a wide range of incident angles, to increase the backscattering field pattern.

Far field pattern of semi-elliptic channel loaded with impedance

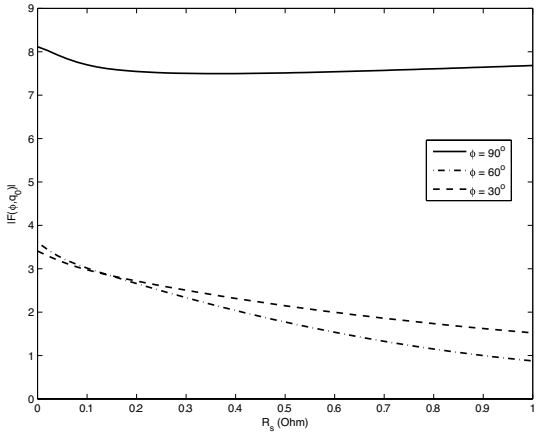

Figure 8. Far field pattern for loaded semi-elliptic channel with $\epsilon = 2\epsilon_0$, $a_2 = 0.7\lambda_0$, $a_1 = \lambda_0$, $e = 0.5$ versus surface resistance.

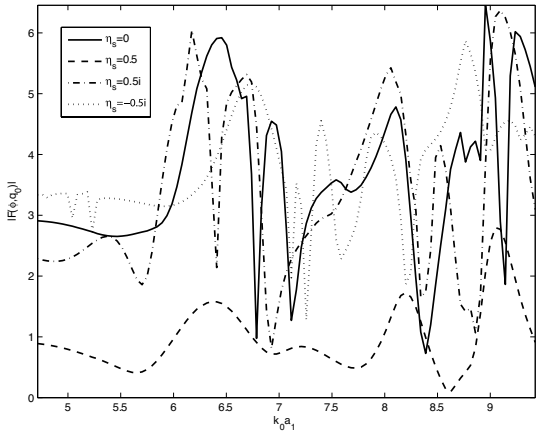

Figure 9. Far field pattern for loaded semi-elliptic channel with $\epsilon = 2\epsilon_0$, $a_2 = 0.7\lambda_0$, $e = 0.5, \phi_0 = 45^\circ$ versus channel electrical size.

core versus reactive coating ($\eta_s = iX_s$) and resistive coating ($\eta_s = R_s$), are depicted in, respectively, Fig. 7 and Fig. 8 for three different observation angles. The resonant-like behavior in Fig. 7 may be attributed to interference of the surface wave with the wave reflected back at the front of cylinder [12]. The resistive coating, however, reduces the far field pattern monotonically. As Fig. 8 shows resistive coating may be used to reduce substantially the interaction of channel

with adjacent EM structures.

Dependance of backscattered far field pattern of loaded semi-elliptic channel on channel electrical size for different coatings are depicted in Fig. 9. The result demonstrates that both magnitude and width of the resonance depend on coating parameters. Resistive coating has the least backscattering magnitude of all results shown.

APPENDIX A. EXPANSION OF NORMALIZATION INTEGRALS

Since angular Mathieu functions with different parameters are not fully orthogonal, some normalization integrals may occur. Expansion of such integrals over $[0, 2\pi]$ interval in terms of Mathieu expansion coefficients were treated in [13]. In problems involving boundary conditions over half ellipse, normalization integrals occur on $[0, \pi]$ interval which can be computed by Mathieu expansion coefficients as follows

$$I_{mn}^{ss}(q_1, q_2) = \begin{cases} \dfrac{\pi}{2} \displaystyle\sum_{k=1,3,\ldots} B_k^m(q_1) B_k^n(q_2), & m,n \text{ odd}; \\ \dfrac{\pi}{2} \displaystyle\sum_{k=2,4,\ldots} B_k^m(q_1) B_k^n(q_2), & m,n \text{ even}; \\ 0, & \text{otherwise}. \end{cases} \tag{A1}$$

$$I_{mn}^{sc}(q_1, q_2) = \begin{cases} \displaystyle\sum_{p=2,4,\ldots} \sum_{k=1,3,\ldots} \frac{2p}{p^2 - k^2} B_p^m(q_1) A_k^n(q_2), & m \text{ even}, n \text{ odd}; \\ \displaystyle\sum_{p=1,3,\ldots} \sum_{k=0,2,\ldots} \frac{2p}{p^2 - k^2} B_p^m(q_1) A_k^n(q_2), & m \text{ odd}, n \text{ even}; \\ 0, & \text{otherwise}. \end{cases} \tag{A2}$$

where

$$I_{mn}^{sc}(q_1, q_2) = \int_0^{\pi} se_m(v, q_1)\, ce_n(v, q_2)\, dv \tag{A3}$$

$$I_{mn}^{ss}(q_1, q_2) = \int_0^{\pi} se_m(v, q_1)\, se_n(v, q_2)\, dv \tag{A4}$$

These expressions are also valid for complex parameter case.

REFERENCES

1. Hinders, M. K. and A. D. Yaghjian, "Dual-series solution to scattering from a semicircular channel in a ground plane," *IEEE Microwave Guided Wave Lett.*, Vol. 1, No. 9, 239–242, 1991.
2. Park, T. J., H. J. Eom, W.-M. Boerner, and Y. Yamaguchi, "TE plane wave scattering from a dielectric-loaded semi-circular trough in a conducting plane," *J. Electromagnetic Waves Applicat.*, Vol. 7, 235–245, 1993.
3. Byun, W. J., J. W. Yu, and N. H. Myung, "TM scattering from hollow and dielectric filled semielliptic channel with arbitrary eccentricity in a perfectly conducting plane," *IEEE Trans. Microwave Theory Tech.*, Vol. 46, No. 9, 1336–1339, 1998.
4. Shen, T., D. Dou, and Z. Sun, "Gaussian beam scattering from a semicircular channel in a conducting plane," *J. Electromagnetic Waves Applicat.*, Vol. 16, 67–85, 1997.
5. Ragheb, H. A., "Electromagnetic scattering from a coaxial dielectric circular cylinder loading a semi channel gap in a ground plane," *IEEE Trans. Microwave Theory Tech.*, Vol. 43, No. 6, 1303–1309, 1995.
6. Hamid, A.-K., "Electromagnetic scattering from a dielectric coated conducting elliptic cylinder loading a semi-elliptic channel in a ground plane," *J. of Electromagn. Waves and Appl.*, Vol. 19, No. 2, 257–269, 2005.
7. Senior, T. B. and J. L. Volakis, "Scattering by gaps and cracks," *IEEE Trans. Antennas Propag.*, Vol. 37, 744–750, 1989.
8. Xiao, J.-K. and Y. Li, "Analysis of method of lines for a novel open truncated circular-groove guide," *J. of Electromagn. Waves and Appl.*, Vol. 19, No. 13, 1795–1805, 2005.
9. Stratton, J. A., *Electromagnetic Theory*, McGraw-Hill, New York, 1941.
10. Abramovitz, M. and I. A. Stegan, *Handbook of Mathematical Functions*, Dover, New York, 1970.
11. Uslenghi, P. L. E., "High frequency scattering from a coated cylinder," *Can. J. Phys.*, Vol. 42, 2121–2128, 1964.
12. Sebak, A. R., "Scattering from dielectric-coated impedance elliptic cylinder," *IEEE Trans. Antenna and Propagation*, Vol. 48, No. 10, 1574–1579, 2000.
13. Angiulli, G., "Radiation from dielectric coated elliptic conducting cylinder by assigned electric current distribution," *Progress In Electromagnetics Research*, PIER 57, 131–149, 2006.